Anomalous Absorption of High-Energy Green Laser Light in High-Z Plasmas

S. H. Glenzer,[1] W. Rozmus,[2,3] V. Yu. Bychenkov,[4] J. D. Moody,[1] J. Albritton,[1] R. L. Berger,[1] A. Brantov,[4]
M. E. Foord,[1] B. J. MacGowan,[1] R. K. Kirkwood,[1] H. A. Baldis,[2] and E. A. Williams[1]

[1]*L-399, Lawrence Livermore National Laboratory, University of California, P.O. Box 808, Livermore, California 94551*
[2]*Institute for Laser Science Applications, University of California, Livermore, California 94550*
[3]*Department of Physics, University of Alberta, Edmonton, Alberta, Canada T6G2J1*
[4]*P. N. Lebedev Physics Institute, Russian Academy of Sciences, Moscow 117924, Russia*

(Received 5 October 2001; published 24 May 2002)

We observe strong anomalous absorption of green laser light in mm-scale high-temperature gold plasmas. Both the laser light absorption and the resulting increase of the electron temperature, which was measured independently with Thomson scattering, have been successfully modeled by including enhanced collisions due to heat-flux driven ion acoustic fluctuations. Calculations that include only inverse bremsstrahlung significantly underestimate the experimental laser absorption and the electron temperature.

DOI: 10.1103/PhysRevLett.88.235002 PACS numbers: 52.35.Fp, 52.50.Jm

Understanding of high-energy laser beam absorption in plasmas plays a central role in many recent studies with short pulse lasers and is fundamental to the success of inertial confinement fusion (ICF). In this Letter, we observe strong anomalous absorption of a 527 nm, i.e., 2ω, laser beam in highly ionized gold plasmas. By varying the laser power of a 2ω probe beam over 4 orders of magnitude, we find that laser absorption begins to deviate from predictions of an inverse bremsstrahlung absorption model for intensities of $I \geq 10^{14}$ W cm^{-2}. By further increasing the (vacuum) laser intensity of the probe beam to $I = 8 \times 10^{15}$ W cm^{-2} the absorption rises to a maximum measured value of 50%. Simultaneously, the electron temperature of the plasma rises from $T_e \simeq 900$ eV to 2 keV. Both these parameters are measured independently; the absorption with a full aperture detector for the transmitted laser light [1] and the temperature with Thomson scattering (TS) [2].

The experimental observations are successfully explained in terms of anomalous processes involving ion-acoustic turbulence (IAT) which is excited by the heat-flux driven return current instability. IAT in ICF plasmas has been predicted to be an important process influencing the laser light absorption [3–5], thermal transport [5–8], and growth and saturation of scattering instabilities [9,10]. In spite of the previous work, IAT is still poorly characterized in laser produced plasmas. The theories of anomalous absorption and thermal transport have been incorporated into our absorption model providing good agreement with the experiment and thus one of the most convincing evidences so far for the IAT.

The experiments were performed at the Nova laser facility at the Lawrence Livermore National Laboratory [11]. The facility was a Nd: glass laser operating at 1.055 μm (1ω) and at converted frequencies of 2ω or 3ω. We used one 3ω ($\lambda = 351$ nm) heater beam which was smoothed with a kinoform phase plate to produce the plasma by irradiating a flat gold disk at an angle of 64° to the disk normal. A 1.5-ns-long flat-topped laser pulse with 100 ps rising and falling edges was chosen with a total energy of 3.8 kJ. The focal spot size was measured by two-dimensional plasma x-ray imaging to be 400 μm $\times$ 600 μm indicating a heater beam intensity of $I = 10^{15}$ W cm^{-2} on target.

Figure 1 shows a hard x-ray image from energies $E > 2$ keV of the plasma as measured with a gated microchannel plate detector (gate time 80 ps) at the end of the heating ($t \simeq 1.5$ ns). In addition to the emission close to the target surface where the heater beam has illuminated the Au plate, the plasma corona shows enhanced emission where a second 2ω probe beam (operating at $\lambda_0 = 527$ nm) passed at a distance of 450 μm across the surface of the target.

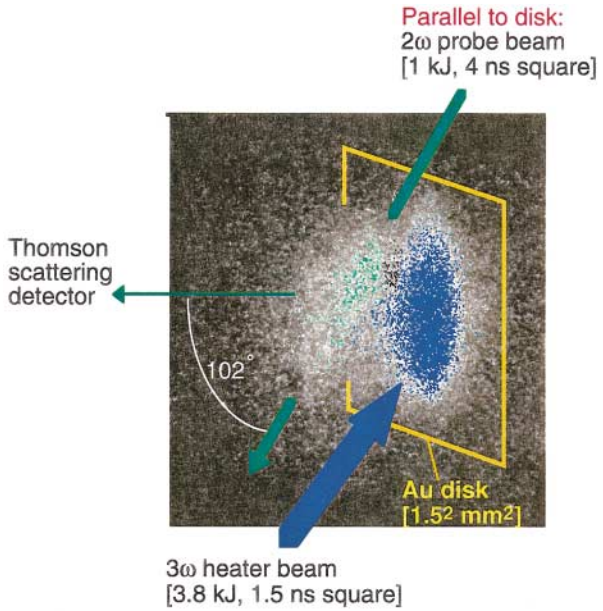

FIG. 1 (color). X-ray emission of the Au plasma for a 2ω probe beam with a (vacuum) intensity of $I = 8 \times 10^{15}$ W cm^{-2}. Also shown is a schematic of the laser beams and diagnostics locations. At this late time ($t = 1.5$ ns) the size of the emission of the focal spot on the Au disk surface has significantly broadened.

The probe beam was focused into the gold blowoff plasma to a spot size of 170 μm giving (vacuum) intensities in the range of $8 \times 10^{11}\ \mathrm{W\,cm^{-2}} < I < 8 \times 10^{15}\ \mathrm{W\,cm^{-2}}$ by varying the laser energy in 4 or 2 ns long square pulses.

The image shown in Fig. 1 was detected at the maximum 2ω probe laser power. The interactions of this beam with the gold plasma were investigated with forward-, side-, and backscattering diagnostics. A frosted silica plate intersected the beam after being transmitted through the plasma providing a full aperture time-resolved measurement of the transmitted laser power and the spatial spreading of the beam [1]. In addition, a full aperture backscatter [12] and near backscatter diagnostics [13] allow measurements of the reflected laser power from the plasma by stimulated Brillouin and Raman scattering. Detectable levels of backscattered light were seen only for laser intensities of $I > 10^{15}\ \mathrm{W\,cm^{-2}}$ with maximum measured values for stimulated Brillouin scattering of 5% and stimulated Raman scattering smaller than 1%. For these high laser intensities, calculations of the laser beam propagation with the code F3D [14] show that the filamentation instability shifts the laser focus closer to its entrance location in the plasma and effectively reduces the vacuum intensity in the plasma center from $I = 8 \times 10^{15}\ \mathrm{W\,cm^{-2}}$ to $2 \times 10^{15}\ \mathrm{W\,cm^{-2}}$. This effect is negligible for lower laser energies.

Figure 2(a) shows the time-resolved measurement of the transmitted laser power from the 2ω beam operating with a 4 ns square pulse at $I = 10^{15}\ \mathrm{W\,cm^{-2}}$. For this measurement a full aperture image of the frosted silica plate was detected with a fast diode and a scope. For the first 800 ps, the plasma had not yet expanded into the path of the probe beam. Consequently, for $0 < t < 0.8$ ns the signal corresponds to 100% transmission. For 0.8 ns $< t <$ 1.5 ns, the Au plasma from the disk surface moves into the path of the probe absorbing the probe light. While the heater beam is on, the absorption is less than 30%. However, for $t > 1.5$ ns when the heater beam turns off, absorption is significant and reaches 42% at $t = 1.75$ ns.

Independently from the absorption measurements, TS measurements of the electron temperature show that the probe is strongly absorbed causing a local temperature rise in the plasma with increasing probe beam power for $t > 1.5$ ns. Figure 2(b) shows three temporally resolved TS spectra that were dispersed by a 1-m spectrometer and detected with a S-20 streak camera. For this purpose, a cylindrical scattering volume located at a distance of 450 μm from the center of the disk surface was imaged onto the entrance slit of the spectrometer. The length of the TS volume is determined by the imaging optics ($f/10$) and is 70 μm for the 1.5 magnification and 100 μm detector slit size. The scattering angle was chosen to be $\theta = 102°$. The streak images show two intense ion acoustic peaks in which the frequency separation is proportional to $\sqrt{ZT_e}$ where Z is the averaged charge state of the Au ions and T_e the electron temperature of the plasma [2,15]. The three measurements shown have significantly different probe beam energies. The comparison of the frequency separation of the two ion acoustic peaks clearly indicates no probe laser heating for the duration of the heater beam, $t \leq 1.5$ ns (even for a probe laser energy of 1 kJ), but strong heating by the energetic probe ($E \geq 30$ J) when the heater beam turns off for $t > 1.5$ ns.

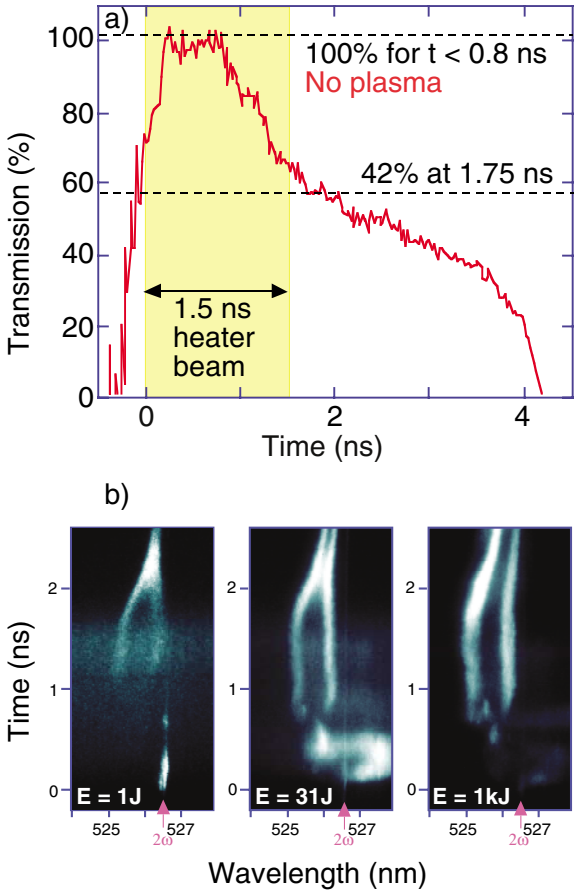

FIG. 2 (color). (a) Example of a time-resolved measurement of the transmitted laser beam for $I = 1 \times 10^{15}\ \mathrm{W\,cm^{-2}}$. (b) Example of TS measurements for three probe laser energies.

For small probe laser energies there is no significant heating by the probe, and the plasma cools down to $T_e \sim$ 900 eV at $t = 1.75$ ns. This time was chosen to calculate T_e from the TS spectra because (1) the absorption data show a quasi-steady-state behavior for ~250 ps, (2) there are density measurements [15], and (3) we were able to confirm with the gated optical imager that the diode measured the full aperture of the transmitted laser light. At higher energies the 2ω probe heats and modifies the underdense plasma [Fig. 2(b)]. The damping of ion acoustic waves in a gold plasma is very small due to the high ionic charge, $30 \leq Z \leq 50$. This gives a low threshold value for the return current ion acoustic instability driven by the temperature gradient, which itself is produced by the localized plasma heating. The theoretical description in the geometry of a laser hot spot has been discussed before using Fokker-Planck simulations [16], by nonlinear weak

turbulence calculations [9], or using analytical solutions to the linearized kinetic equations [17].

The approximate expression for a linear growth rate of the return current instability reads [17]

$$\gamma = \sqrt{\frac{\pi}{8}}\,\omega_{pi}\,\frac{k\lambda_D}{(1 + k^2\lambda_D^2)^{3/2}}\,\frac{\lambda_{ei}}{L}, \tag{1}$$

where k is the characteristic wave number of the unstable mode, λ_D is the Debye length, λ_{ei} the electron-ion collision mean free path, and L is the temperature gradient scale length. The growth rate (1) reaches a maximum for $k\lambda_D = 0.71$. Taking as typical plasma parameters, $T_e = 1500$ eV, $n_e = 10^{20}$ cm^{-3}, $Z = 40$, one finds $\lambda_{ei} = 10$ μm and $\gamma = 1.46 \times 10^{12}\lambda_{ei}/L$ s^{-1}. Calculating the damping rate, γ_1 [17] due to electron Landau damping and ion-ion collisions for the same parameters and $T_i = 1000$ eV, one obtains $\gamma_1 = 4.5 \times 10^{10}$ s^{-1}, which sets the threshold condition for the instability at $L = 32\lambda_{ei}$, i.e., for $L \approx 300$ μm. With a more realistic gradient scale length of $L = 100$ μm, the instability develops over the time of tens of picoseconds which is consistent with more refined nonlocal kinetic calculations [17].

The initial exponential growth of the instability, described by Eq. (1), continues until collective fluctuations have sufficient amplitude to modify the plasma response and consequently saturate the instability. In particular, IAT enhances the electron collisionality, which leads to increased resistivity and slowing down of the electron-ion drift. This mechanism is described by the quasilinear theory, which is included in our model of the IAT together with the induced scattering of ion acoustic waves on ions. In the quasistationary state, the electron distribution function is close to the marginal stability condition and further evolution of the IAT spectrum is due to induced scattering on ions. This results in the Kadomtsev-Petviashvili distribution [18] of the IAT spectral energy density and angular distribution defined by the so-called turbulent Knudsen number, K_N [5],

$$K_N \approx 12\,\frac{T_i}{ZT_e}\,\frac{1}{m_e c_s \omega_{pi}}\left|\frac{dT_e}{dr}\right|, \tag{2}$$

where r is the radial variable in the cylindrical geometry considered in the model. For the conditions described under Eq. (1) we have $K_N \approx 1$, and K_N varies in the range of $0.1 < K_N < 10$ for the various 2ω probe beam intensities of the experiment. K_N can be used (cf. also Ref. [9]) to define the anomalous collision frequency,

$$\nu_{\rm an} = 0.04\omega_{pi}\,\frac{ZT_e}{T_i}\left(\frac{1 + 9K_N^2}{K_N^2 + \ln^2(1/K_N)}\right)^{1/2}, \tag{3}$$

which is responsible for the enhanced absorption of the laser light.

The enhanced electron collisionality affects all transport processes, in particular, thermal conduction, which is modeled in terms of the inhibition factor, f, in the following expression for the anomalous heat flux:

$$q_{\rm an} = -f n_e T_e v_{\rm the}, \qquad f = \left(\frac{dT_e}{dr}\Big/\left|\frac{dT_e}{dr}\right|\right)0.18\sqrt{\frac{Z}{A}}\,(1 + 1.6\sqrt{K_N}), \tag{4}$$

where A is the atomic number and $v_{\rm the}$ electron thermal velocity. In the plasma heating model, we combine the e-i collision frequency, ν_{ei}, with the anomalous one, $\nu_{\rm an}$, in one expression for the effective collision frequency, $\nu_{\rm eff} = \nu_{\rm an} + \nu_{ei}$. Similarly, an electron heat flux, q, is approximated by $1/q = 1/q_{\rm SH} + 1/q_{\rm an}$, where $q_{\rm SH} = \xi(Z) \times n_e v_{\rm the} T_e \lambda_{ei}/L$ is the Spitzer-Härm expression for the heat flux and ξ accounts for the effect of e-e collisions [17].

The experimental data show a quasistationary state of the plasma for the period between 1.6 and 2 ns (cf. Fig. 2). Therefore, we balance the absorbed laser power into the plasma, $\mathcal{A}$, by the heat conduction, radiative losses, $\mathcal{R}$, and the convection away from the region in the center of the laser beam. Assuming cylindrical symmetry, these processes are described by the following equation:

$$\frac{1}{r}\,\frac{d}{dr}\,(rq) = \mathcal{A} - \mathcal{R} - \frac{3}{2}\,n_e u\,\frac{dT_e}{dr} - n_e T_e\,\frac{1}{r}\,\frac{d}{dr}\,(ru), \tag{5}$$

where u is the transverse flow velocity and we have neglected small electron energy losses due to the excitation of IAT. The absorbed power per unit volume reads

$$\mathcal{A} = \nu_{\rm eff} I_0 \exp(-r^2/a^2)\,\frac{1}{c}\,\frac{n_e}{n_c}\,\exp\left(-\nu_{\rm eff}\,\frac{n_e}{n_c}\,\frac{x}{c}\right). \tag{6}$$

This is a reasonable approximation until self-focusing modifies the energy distribution at high laser intensities ($I_0 > 10^{15}$ W/cm^2). We take $a = 80$ μm and x is the path length to the TS volume, $x \approx 0.5$ mm.

Figure 3 compares T_e from the TS measurements with the IAT model [Eqs. (5) and (6)] and the inverse bremsstrahlung model. The magnitude of the radiation losses term $\mathcal{R}$ in (5) and Z are obtained from detailed atomic models with inclusion of processes such as dielectronic recombination [15]. Using the predictions of the nonlocal thermodynamic equilibrium atomic kinetic scheme that involves two-electron transitions [19], we have calculated Z and inferred T_e from the frequency separation of the ion acoustic wave resonances [Fig. 2(b)]. We observe good agreement of the TS results with the IAT model except the last data point where F3D calculations indicate that self-focusing (filamentation) starts to play a role increasing the potential error in the identification of the beam intensity at the TS volume as well as the error of T_e. Some discrepancies with the experimental data at $I \approx 10^{14}$ W/cm^2, i.e., close to the threshold value for the ion wave instability could result from *ad hoc* transitions in the theoretical model between collisional regime and fully developed IAT. In particular, the increase of the

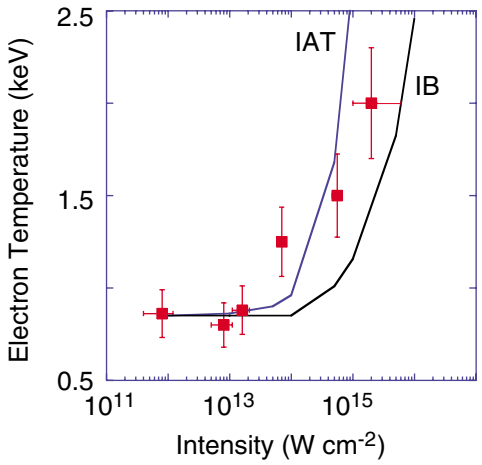

FIG. 3 (color). Electron temperatures measured by Thomson scattering as a function of probe laser intensity (squares). Also shown are theoretical calculations from the anomalous absorption (IAT) and from the inverse bremsstrahlung absorption (IB) models.

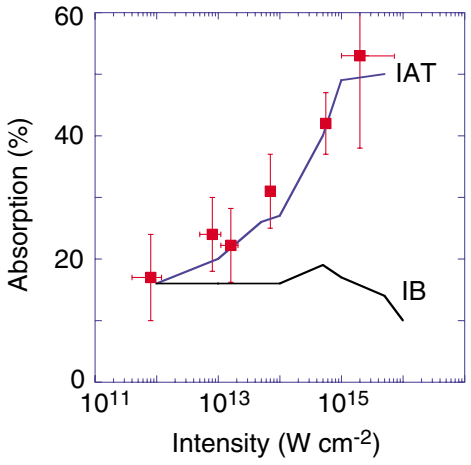

FIG. 4 (color). Absorption for various 2ω probe beam intensities. The comparison with two models show that inverse bremsstrahlung absorption (IB) is not sufficient to explain the measurements (squares). Good agreement can be seen when including ion acoustic turbulence (IAT).

experimental T_e data at smaller laser intensities agrees well with the IAT model and not with the predictions from the inverse bremsstrahlung absorption model.

In Fig. 4 we demonstrate that the absorption is well modeled by our enhanced electron collision term in the presence of the IAT. The measured absorption increases rapidly with increasing laser intensity and plasma temperature from 15% up to 50%. In this figure, the obvious discrepancies between the experimental data and the inverse bremsstrahlung absorption model clearly indicates anomalous absorption. Good agreement can be seen with the calculated total laser probe absorption, A, that uses the following expression:

$$A = 1 - 2\int_0^\infty d\rho\, \rho \exp\left(-\rho^2 - \frac{l_{abs}\nu_{\text{eff}}}{c}\frac{n_e}{n_c}\right), \quad (7)$$

where $\rho = r/a$, $l_{abs} = 1$ mm. The temperature profile and the level of ion acoustic fluctuations in Eq. (7) is calculated from the stationary model (5).

In summary, we have shown that high-Z gold plasmas display anomalous behavior efficiently absorbing 2ω laser light with a rate that increases with laser intensity and plasma temperature. For the intensities $I > 10^{14}$ W/cm^2 the absorption coefficient increases with electron temperature reaching values of 50% at $I = 2 \times 10^{15}$ W/cm^2 and $T_e = 2$ keV. This behavior is explained in terms of the heat-flux driven ion acoustic instability and enhanced electron collision frequency. Our modeling is motivated by early ideas in ICF research [3,4,7]; however, it introduces IAT on the scale of a single laser hot spot, thus potentially affecting modeling of plasma transport and interaction physics in large scale underdense plasmas created by randomized laser beams.

This work was performed under the auspices of the U.S. Department of Energy by University of California Lawrence Livermore National Laboratory under Contract No. W-7405-ENG-48. W. R. has been partially supported by the Natural Science and Engineering Research Council. V. Yu. B. has been partially supported by the Russian Foundation for Basic Research (Grant No. 00-02-16063).

[1] J. D. Moody *et al.,* Rev. Sci. Instrum. **70**, 677 (1999).
[2] S. H. Glenzer *et al.,* Phys. Plasmas **6**, 2117 (1999).
[3] W. M. Manheimer *et al.,* Phys. Rev. Lett. **38**, 1135 (1977).
[4] R. J. Faehl and W. L. Kruer, Phys. Fluids **20**, 55 (1977).
[5] V. Yu. Bychenkov *et al.,* Phys. Rep. **164**, 119 (1988).
[6] D. R. Gray and J. D. Kilkenny, Plasma Phys. Controlled Fusion **22**, 81 (1980).
[7] R. I. Bickerton, Nucl. Fusion **13**, 457 (1973).
[8] W. M. Manheimer, Phys. Fluids **20**, 265 (1977).
[9] W. Rozmus *et al.,* Phys. Rev. E **50**, 4005 (1994).
[10] A. V. Maximov *et al.,* Phys. Plasmas **3**, 1689 (1996).
[11] E. M. Campbell *et al.,* Laser Part. Beams **9**, 209 (1991).
[12] B. J. MacGowan *et al.,* Phys. Plasmas **3**, 2029 (1996).
[13] R. K. Kirkwood *et al.,* Rev. Sci. Instrum. **68**, 636 (1997).
[14] R. L. Berger *et al.,* Phys. Plasmas **5**, 4337 (1998).
[15] S. H. Glenzer *et al.,* Phys. Rev. Lett. **82**, 97 (1999).
[16] V. T. Tikhonchuk, W. Rozmus, V. Yu. Bychenkov, C. E. Capjack, and E. Epperlein, Phys. Plasmas **2**, 4169 (1995).
[17] A. V. Brantov, V. Yu. Bychenkov, and W. Rozmus, Phys. Plasmas **8**, 3558 (2001).
[18] A. A. Galeev and R. Z. Sagdeev, in *Handbook of Plasma Physics,* edited by A. A. Galeev and R. N. Sudan (North-Holland, Amsterdam, 1984), Vol. 2, p. 271.
[19] J. R. Albritton and B. G. Wilson, Phys. Rev. Lett. **83**, 1594 (1999).